

Dalton Transactions

Accepted Manuscript



This is an *Accepted Manuscript*, which has been through the Royal Society of Chemistry peer review process and has been accepted for publication.

Accepted Manuscripts are published online shortly after acceptance, before technical editing, formatting and proof reading. Using this free service, authors can make their results available to the community, in citable form, before we publish the edited article. We will replace this *Accepted Manuscript* with the edited and formatted *Advance Article* as soon as it is available.

You can find more information about *Accepted Manuscripts* in the [Information for Authors](#).

Please note that technical editing may introduce minor changes to the text and/or graphics, which may alter content. The journal's standard [Terms & Conditions](#) and the [Ethical guidelines](#) still apply. In no event shall the Royal Society of Chemistry be held responsible for any errors or omissions in this *Accepted Manuscript* or any consequences arising from the use of any information it contains.

ARTICLE

Exemplary Relationship between the Extent of Cofacial Aggregation and Fluorescence Quantum Yield as Exhibited by Quaternized Amphiphilic Phthalocyanines

Cite this: DOI: 10.1039/x0xx00000x

Received 00th January 2012,
Accepted 00th January 2012

DOI: 10.1039/x0xx00000x

www.rsc.org/

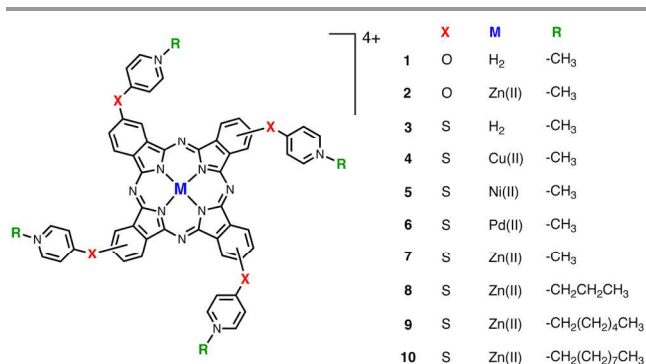
Thiago Teixeira Tasso,^a Yasuhiro Yamasaki,^{*b} Taniyuki Furuyama,^a
and Nagao Kobayashi^{*a}

The aggregation equilibrium of a series of positively-charged water-soluble phthalocyanines (Pcs) was studied in aqueous solution by means of absorption and fluorescence techniques. The aggregation equilibrium in water depends on the bridging atoms between the pyridyl groups and the Pc core, and on the central metal of the Pcs, while *N*-alkyl groups are virtually uninvolved in the aggregation properties. Thus, in the water-methanol mixture, the aggregation tendency increased in the order of Zn < Cu ≤ Ni, Pd when the ligand is the same, while the bridging element sulfur gives much more propensity for aggregation compared to oxygen. The fluorescence quantum yields of the Pcs showed an excellent correlation with the extent of aggregation.

Introduction

Phthalocyanines (Pcs) and related cyclic tetrapyrrolic macrocycles comprise a highly conjugated π -electron structure which confers them with special properties useful for applications in a wide range of areas. Versatility also plays an important role in the features of these chromophores, since their physicochemical properties can be tuned via insertion of different substituents and central elements into the ring.¹ Although Pcs are usually insoluble in most organic solvents, this problem can be overcome by introducing different substituent groups at the α or β positions of the peripheral moieties. Water solubility, required for many applications in various fields, is most frequently achieved by the use of negatively-charged substituents, such as sulfoxyl (SO_3^-) and/or carboxyl (COO^-) groups.² Materials which have intense fluorescence in water can become promising candidates for the design of novel biomarkers and photosensitizers. However, ionic Pcs are known to aggregate easily via π - π stacking of the rings, leading to disadvantages, such as fluorescence quenching or loss of catalytic activity.³ Hence, the control of the aggregation and fluorescence properties in water is a significant topic in material science. In this context, we have designed a series of water-soluble Pcs containing quaternized pyridyl (pyridinium) groups (Scheme 1), and investigated their aggregation equilibrium in solution. Pyridyl groups are easily quaternized, to yield positively-charged species, while positively-charged Pcs also show a higher tendency for DNA binding and improved uptake by bacterial cells.⁴ The influence of the chemical structure is crucial for the aggregation equilibrium, but up to now, quantitative analysis of separate variables has been mainly restricted to sulfonic or non-ionic

substituents.^{1a, 5} The structure of the pyridinium Pcs includes three elements in addition to the Pc core: (1) bridging atoms (**X**), (2) central metal (**M**), and (3) *N*-alkyl groups (**R**). The aggregation behavior of aryloxy-derivatized metalloPcs in toluene solution was previously investigated, showing that their behavior is different from metal to metal.⁶ We recently synthesized iron and cobalt water-soluble Pcs, and found that their aggregation properties also depended on the central metal.⁷ To investigate these characteristics further, Pcs with different bridging atoms (compounds **1-2** (O) vs. **3-10** (S)), different central metals with the same substituents (compounds **3-7**), and different *N*-alkyl groups with the same central metal (compounds **7-10**) have been prepared and analyzed. In particular, we have found an exemplary linear relationship between dimerization and the fluorescence quantum yield. Although it has long been postulated that fluorescence decreases on aggregation, such a precise relationship as shown here has not been previously proven.



Scheme 1 Structures of the Pcs in this study.

Experimental

Materials and methods

All chemicals were analytical grade and purchased from commercial sources. The solvents were purified by distillation and all other reagents were used without further purification. The ¹H NMR and the ¹³C NMR spectra were measured at 300.4 MHz and 75.45 MHz, respectively, using JEOL JNM-AL 300 equipment. The UV-vis spectra were obtained by a JASCO V-570 spectrophotometer and the IR spectra were measured using a JEOL JIR-SPX-60S spectrophotometer. Fluorescence spectra were obtained on a HITACHI F-4500 spectrofluorometer. Absolute fluorescence quantum yields were measured on a Hamamatsu C9920-03G calibrated integrating sphere system. The FD MS spectra were measured in the positive and direct-induced mode using a JEOL JMS 600 spectrometer. Melting point measurements of the phthalonitriles were carried out with the Micro Melting Point Apparatus MP-500D produced by YANACO Instrument Co. Ltd.

Synthetic procedures

4-Pyridylsulphanylphthalonitrile 4-Hydroxypyridine (10.0 g, 0.10 mol), dry K₂CO₃ (29.1 g) and 200 mL of dried DMF were placed in a 1 L rounded-bottomed flask equipped with an overhead stirrer, rubber seal and a dropping funnel in which the solution of 4-nitro-2,3-dicyanobenzene (0.10 mol) in 100 mL of DMF was placed. After a stream of nitrogen was passed through the slurry to remove oxygen, the DMF solution was added dropwise over 18 h. The resulting mixture was poured into 3 L of water under vigorous stirring, filtered and the solid washed with hot water and dried *in vacuo*. The pale-yellow solid was dispersed in 1 L of CHCl₃ and the resulting mixture was filtered. Evaporation of the solution yielded 3.76 g (16.4%) of the desired nitrile. GC-MS: *m/z* = 221. 300 MHz ¹H NMR (CDCl₃) δ (ppm): 8.65 (dd, *J* = 4.8 Hz, *J* = 1.5 Hz, 2H), 7.86 (d, *J* = 8.7, 1H), 7.48 (d, *J* = 2.7 Hz, 1H), 7.41 (dd, *J* = 8.7 Hz, *J* = 2.7 Hz, 1H), 7.00 (dd, *J* = 4.8 Hz, *J* = 1.5 Hz, 2H). 75 MHz ¹³C NMR (CDCl₃) δ (ppm): 161.3, 158.7, 152.4, 135.7, 123.7, 123.5, 118.0, 114.8, 114.4, 114.0, 111.1. FTIR (KBr pellet, cm⁻¹): 3052, 3031(m), 2968, 2360(w), 2231(s), 1653, 1606(m), 1578, 1562, 1483, 1414, 1284, 1250, 1200(vs), 1090, 951, 881, 858(s); mp 144.1-146.9°C.

4-Pyridyloxyphthalonitrile 4-Nitrophthalonitrile (38.9 g, 0.22 mol), dry K₂CO₃ (40.0 g) and 300 mL of dried DMF were placed in a 1 L rounded-bottomed flask equipped with an overhead stirrer and rubber seal. After a stream of nitrogen was passed through the slurry to remove oxygen, 4-pyridinethiol

(25.0 mL, 0.22 mol) was added to the mixture and stirred at room temperature. After 8 hours, more K₂CO₃ (40.0 g) was added and the mixture stirred for additional 15 h. The resulting mixture was poured into 3 L of water under vigorous stirring, filtered and the solid washed with hot water and dried *in vacuo* to yield 40.0g (75%) of the desired yellow product. GC-MS: *m/z* = 237. 300 MHz ¹H NMR (CDCl₃) δ (ppm): 8.62 (d, *J* = 4.6 Hz, 2H), 7.79-7.65 (m, 3H), 7.25(d, *J* = 4.6, 2H). 75 MHz ¹³C NMR (CDCl₃) δ(ppm): 150.6, 142.7, 142.0, 134.3, 134.0, 125.1, 117.0, 114.8, 114.5, 114.1. FTIR (KBr pellet, cm⁻¹): 3089, 3043(w), 3003, 2231(s), 1572(vs), 1483, 1410(s), 1279, 1221, 1082(w), 818, 708, 530(s); mp 148.0-149.0°C.

Tetrakis[4-(iodo-*N*-methylpyridinium)oxy]phthalocyanine

(1) 4-pyridyloxyphthalonitrile 1.959 g (8.86 mmol) and 1-pentanol (20 mL) were placed in a 100 mL 3-necked flask equipped with a condenser and rubber seal. After purging nitrogen, 1.48 g of DBU (9.73 mmol) were added through a syringe and the resulting mixture was stirred for 8 hours at 105-110°C. After the solvent was removed, addition of acetone gave a blue precipitate, which was filtered, washed with NaOH 1.0 M, water and acetone. After drying *in vacuo*, 0.828 g of tetrakis(4-pyridyloxy)phthalocyanine was obtained (53.9%). For the methylation reaction, the free-base phthalocyanine (0.056 g, 0.05 mmol), 1.0 mL of methyl iodide and 10 mL of DMF were placed in a 100 mL pressure-resistant reactor and the mixture was stirred at 70-80°C for 30 minutes. After removal of the DMF and methyl iodide by evaporation, addition of acetone to the resultant oil yielded a blue precipitate, which was washed with CHCl₃ and acetone and dried *in vacuo* overnight to yield 0.078 g of title compound (84.4%). *Anal.* Calcd for C₅₆H₄₂I₄N₁₂O₄: C, 46.24; H, 2.91; N, 11.55. Found: C, 46.06; H, 3.18; N, 11.46. FTIR (KBr pellet, cm⁻¹): 3437(m), 3014(w), 1645(vs), 1614(s), 1579(m), 1512(vs), 1471(s), 1421, 1398(m), 1398(m), 1308, 1284, 1207, 1113, 1092(s), 1011, 930, 835, 746, 505(m).

Tetrakis[4-(iodo-*N*-

methylpyridinium)oxy]phthalocyaninato zinc(II) (2) 4-pyridyloxyphthalonitrile (0.664 g, 3.0 mmol), anhydrous zinc acetate (2.75 g, 1.5 mmol), 1-pentanol (6 mL) were placed in a 50 mL 3-necked flask equipped with a condenser and a rubber seal. After purging nitrogen, DBU (0.457 g, 3.0 mmol) was added through a syringe and the resulting mixture was stirred for 8 h at 105-110°C. After evaporating the solvent in a rotary evaporator, addition of acetone to the product yielded a blue precipitate, which was filtered, washed with NaOH solution (1 M), water and acetone. After drying *in vacuo* overnight, 0.63 g of tetrakis(4-pyridyloxy)phthalocyaninato zinc(II) was obtained (37.3%). For methylation of the pyridyl rings, the obtained phthalocyanine (0.097 g, 0.07 mmol), methyl iodide (1.0 mL), and DMF 10 mL were placed in a 100 mL pressure-resistant reactor and the mixture was stirred at 80°C for 30 min. After evaporation of the DMF and methyl iodide excess, the product was precipitated with acetone, filtered, washed with CHCl₃ and acetone and dried *in vacuo* overnight to yield 0.15 g of title compound (95.5%). *Anal.* Calcd for C₅₆H₄₀I₄N₁₂O₄Zn: C, 44.31; H, 2.66; N, 11.07. Found: C, 43.95; H, 3.14; N, 10.95.

FTIR (KBr pellet, cm^{-1}): 3419(m), 3032(w), 1643(s), 1608(m), 1581(m), 1512(vs), 1487(w), 1464(s), 1333, 1306(m), 1286(vs), 1205(s), 1088, 1047, 945(m), 835, 748, 511(w).

Tetrakis[4-(iodo-*N*-methylpyridinium)thio]phthalocyanine (3) 4-Pyridylthiophthalonitrile 4.746 g (20.0 mmol) and 1-pentanol (50 mL) were placed in a 100 mL 3-necked flask equipped with a condenser and rubber seal. After purging nitrogen, 3.05 g of DBU (20.0 mmol) were added through a syringe and the resulting mixture was stirred for 8 hours at 105–110°C. After the solvent was removed, addition of acetone gave a blue precipitate, which was filtered, washed with NaOH 1.0 M, water and acetone. After drying *in vacuo*, 1.72 g of tetrakis(4-pyridylthio)phthalocyanine was obtained (36.2%). For the methylation reaction, the free-base phthalocyanine (0.061 g, 0.05 mmol), 1.0 mL of methyl iodide and 10 mL of DMF were placed in a 100 mL pressure-resistant reactor and the mixture was stirred at 70–80°C for 30 minutes. After removal of the DMF and methyl iodide by evaporation, addition of acetone to the resultant oil yielded a blue precipitate, which was washed with CHCl_3 and acetone and dried *in vacuo* overnight to yield 0.061 g of title compound (92.0%). *Anal.* Calcd for $\text{C}_{56}\text{H}_{42}\text{I}_4\text{N}_{12}\text{S}_4$: C, 44.28; H, 2.79; N, 11.07. Found: C, 44.36; H, 2.87; N, 10.92. FTIR (KBr pellet, cm^{-1}): 3437(w), 3005(w), 1628(vs), 1549(w), 1491(s), 1444, 1406, 1302(m), 1192, 1132(m), 1105(s), 1011(s), 895, 814(m), 741(s), 698, 673, 634(w), 482(m).

Tetrakis[4-(iodo-*N*-methylpyridinium)thio]phthalocyaninato copper(II) (4) 4-Pyridylthiophthalonitrile (0.95 g, 4.0 mmol), $\text{CuSO}_4 \cdot 2\text{H}_2\text{O}$ (2.72 g, 1.5 mmol), 1-pentanol (6 mL) were placed in a 50 mL 3-necked flask equipped with a condenser and a rubber seal. After purging nitrogen, DBU (0.61 g, 4.0 mmol) was added through a syringe and the resulting mixture was stirred for 8 h at 110°C. After evaporating the solvent in a rotary evaporator, addition of acetone to the product yielded a blue precipitate, which was filtered, washed with NaOH solution (1 M), water and acetone. After drying *in vacuo* overnight, 0.63 g of tetrakis(4-pyridylthio)phthalocyaninato copper(II) was obtained (62.3%). For methylation of the pyridyl rings, the obtained phthalocyanine (0.098 g, 0.07 mmol), methyl iodide (1.0 mL), and DMF 10 mL were placed in a 100 mL pressure-resistant reactor and the mixture was stirred at 80°C for 30 min. After evaporation of the DMF and methyl iodide excess, the product was precipitated with acetone, filtered, washed with CHCl_3 and acetone and dried *in vacuo* overnight to yield 0.14 g of title compound (91.1%). *Anal.* Calcd for $\text{C}_{56}\text{H}_{40}\text{CuI}_4\text{N}_{12}\text{S}_4$: C, 42.56; H, 2.55; N, 10.64. Found: C, 42.43; H, 2.76; N, 10.46. FTIR (KBr pellet, cm^{-1}): 3419(m), 3010(w), 1630(vs), 1558(w), 1493(s), 1456, 1394(w), 1311(m), 1196(w), 1146(m), 1105(s), 1045, 920, 816, 746(m), 692.

Tetrakis[4-(iodo-*N*-methylpyridinium)thio]phthalocyaninato nickel(II) (5) The same procedures described for **4** were used for the synthesis of **5**, using instead NiCl_2 as the metal salt. The procedures yielded 0.858 g of tetrakis(4-pyridylthio)phthalocyaninato nickel(II) (85.1%) and 0.1714 g of title compound (99.7%). *Anal.* Calcd

for $\text{C}_{56}\text{H}_{40}\text{I}_4\text{N}_{12}\text{NiS}_4$: C, 42.69; H, 2.56; N, 10.67. Found: C, 42.48; H, 3.06; N, 10.39%. FTIR (KBr pellet, cm^{-1}): 3421(m), 3010(w), 1630(vs), 1552, 1531(w), 1493(s), 1450, 1396(w), 1144(m), 1105(s), 1047, 933, 816, 750(m), 484(m).

Tetrakis[4-(iodo-*N*-methylpyridinium)thio]phthalocyaninato palladium(II) (6) The same procedures described for **4** were used for the synthesis of **6**, using instead $\text{Pd}(\text{OAc})_2$ as the metal salt. The procedures yielded 0.262 g of tetrakis(4-pyridylthio)phthalocyaninato palladium(II) (29.4%) and 0.262 g of title compound (24.8%). *Anal.* Calcd for $\text{C}_{56}\text{H}_{40}\text{I}_4\text{N}_{12}\text{PdS}_4$: C, 41.43; H, 2.48; N, 10.35. Found: C, 41.09; H, 2.73; N, 10.12. FTIR (KBr pellet, cm^{-1}): 3423(m), 3010(w), 1628(vs), 1552(w), 1491(s), 1456(m), 1353(w), 1309(m), 1259, 1194(w), 1149(m), 1105(s), 1045, 932(w), 816, 746(m), 484(m).

Tetrakis[4-(iodo-*N*-methylpyridinium)thio]phthalocyaninato zinc(II) (7) The same procedures described for **4** were used for the synthesis of **7**, using $\text{Zn}(\text{OAc})_2$ as the metal salt. The procedures yielded 0.59 g of tetrakis(4-pyridylthio)phthalocyaninato zinc(II) (58.1%) and 0.15 g of title compound (95.7%). *Anal.* Calcd for $\text{C}_{56}\text{H}_{40}\text{I}_4\text{N}_{12}\text{S}_4\text{Zn}$: C, 42.51; H, 2.55; N, 10.62. Found: C, 42.47; H, 2.77; N, 10.44%. FTIR (KBr pellet, cm^{-1}): 3446(m), 3012(w), 1630(vs), 1489(s), 1458, 1387, 1308, 1142(m), 1105(s), 1043, 908, 816, 744(m), 687, 484.

Tetrakis[4-(iodo-*N*-propylpyridinium)thio]phthalocyaninato zinc(II) (8) Tetrakis(4-pyridylthio)phthalocyaninato zinc(II) (0.0940 g, 4 mmol), 1.0 mL of propyl iodide and 10 mL of DMF were placed in a 100 mL pressure-resistant reactor and the mixture was stirred at 70–80°C for 8 hours. After removal of the DMF and methyl iodide by evaporation, addition of 20 mL of acetone to the resultant oil yielded a blue precipitate, which was washed with CHCl_3 and acetone and dried *in vacuo* overnight to yield 0.1570 g of title compound (99.5%). *Anal.* Calcd for $\text{C}_{64}\text{H}_{56}\text{I}_4\text{N}_{12}\text{S}_4\text{Zn}$: C, 45.36; H, 3.33; N, 9.92. Found: C, 44.46; H, 3.50; N, 10.35. FTIR (KBr pellet, cm^{-1}): 3425(m), 3012, 2960, 2929, 2872(w), 1626(vs), 1573, 1549(w), 1488(s), 1456(m), 1382, 1307, 1180(w), 1140(m), 1101(s), 1041, 908, 831, 814, 769, 760(w), 744(m), 687, 513(w).

Tetrakis[4-(bromo-*N*-hexylpyridinium)thio]phthalocyaninato zinc(II) (9) Same procedure described for **8** were used for the synthesis of **9**, using hexyl bromide instead of propyl iodide. Yield: 0.1344 g (84.5%). *Anal.* Calcd for $\text{C}_{76}\text{H}_{80}\text{Br}_4\text{N}_{12}\text{S}_4\text{Zn}$: C, 54.50; H, 4.81; N, 10.04. Found: C, 53.92; H, 4.54; N, 10.89%. FTIR (KBr pellet, cm^{-1}): 3425(m), 3012, 2960, 2929, 2872(w), 1626(vs), 1573, 1549(w), 1488(s), 1456(m), 1382, 1307, 1180(w), 1140(m), 1101(s) 1041, 908, 831, 814, 769, 760(w), 744(m), 687, 513(w).

Tetrakis[4-(iodo-*N*-nonylpyridinium)thio]phthalocyaninato zinc(II) (10) Same procedure described for **8** were used for the synthesis of **10**, using nonyl iodide instead of propyl iodide. Yield 0.4130 g (98.7%). *Anal.* Calcd for $\text{C}_{88}\text{H}_{104}\text{I}_4\text{N}_{12}\text{S}_4\text{Zn}$: C, 52.04; H, 5.16; N, 8.28. Found: C, 53.65; H, 5.72; N, 6.80.

FTIR (KBr pellet, cm^{-1}): 3429(m), 2997(w), 2953(m), 2921, 2852(s), 1626(vs), 1547(w), 1489(s), 1459(m), 1381, 1308(m), 1182(w), 1139(m), 1099(s) 1074, 1064, 908(m), 829(m), 814, 769, 760(w), 744(m), 687, 513(w).

Results and discussion

The Pcs were synthesized via tetramerization reaction of the respective phthalonitriles and metal salts in *n*-pentanol at 105–110°C. Subsequent quaternization of the pyridyl groups was achieved by reaction with the respective alkyl halides in DMF at 70–80°C, with moderate to high yields. The products were characterized by elemental analysis, MALDI-TOF mass spectrometry, FTIR and UV-vis absorption spectroscopy.

First, we will illustrate the general aggregation properties of the alkylpyridinium Pcs through the spectra of the representative tetrakis[4-(*N*-methylpyridinium)thio]Pc zinc complex **7**. Fig. 1 shows the UV-vis absorption and MCD spectra in pure aqueous and methanol solutions.

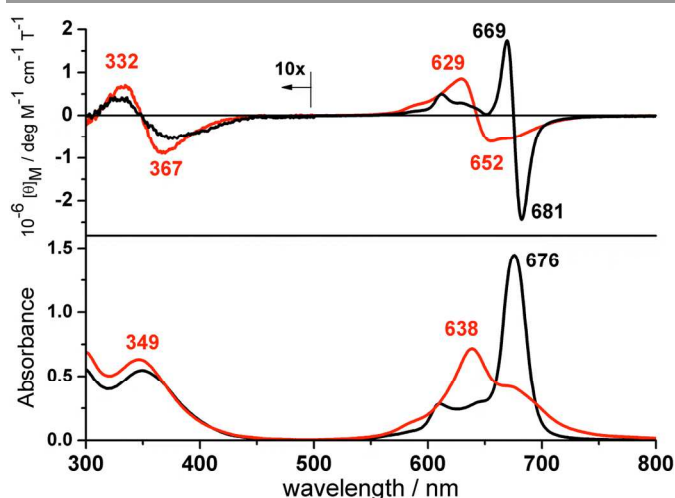


Fig. 1 UV-vis absorption (bottom) and magnetic circular dichroism (top) spectra of compound **7** (ca. 1.0×10^{-5} M) in aqueous (red) and methanol (black) solutions.

In methanol solution, compound **7** shows a single, intense Q absorption band in the 600–700 region and a Soret band at 349 nm, which are typical of unaggregated metalloPcs with D_{4h} symmetry. The MCD spectrum of **7** shows dispersion-type Faraday *A* terms corresponding to both the Soret and Q bands, indicating that the excited states of the chromophore are degenerate. Thus, it is concluded that pyridinium metalloPc exists in the monomeric form in a dilute methanol solution, as supported also by the Lambert-Beer plot of **7**, shown in Fig. S1 (ESI). In contrast, the absorption spectrum in water is markedly different, with a broad peak appearing at 638 nm in the Q band region. This broad, blue-shifted absorption band suggests that **7** forms face-to-face (H-type) aggregates^{1, 8} in water, as similarly observed for the chiral zinc phthalocyanine reported by Jiang *et al.* in concentrated CHCl_3 solutions.⁹ This arrangement is also supported by the Faraday *A* MCD terms, suggesting that the dimer has structures close to either D_{4h} or D_{4d} . The absorption spectra of compound **7** in a series of water/methanol mixtures are shown in Fig. 2a. By increasing the water proportion in the

mixtures, the Q band due to the monomer (at 676 nm) in methanol decreases sharply, with a set of isosbestic points and concomitant increase of the band at 638 nm, until its complete appearance in pure aqueous solution. Since the spectrum in methanol is that of monomeric Pc and a set of isosbestic points is detected by changing water-methanol ratio, the spectrum in water is ascribed to that of a dimer. Fig. 2b shows a plot of the absorbance of both the monomer (676 nm) and dimer Q (638 nm) bands versus the methanol percentage in the mixtures. It is clear that significant disaggregation of **7** occurs in solutions containing more than 40% methanol, and is almost complete at 100% methanol solution. The intersection point between both curves represents the proportion of methanol in which the monomer/dimer ratio in solution is 1:1, which was found to be 71% for **7**. This volume of methanol (I_M) indicates the aggregation propensity in water (a higher I_M value indicates a stronger tendency for macrocycles to aggregate in solution). In Figure 2b, the corresponding plots for **2** are also included. While the only difference between **7** and **2** is the bridging element, S for **7** and O for **2**, the I_M value for **2** is 49%. Although S and O are very close in the periodic table, the bridging element significantly affects the aggregation behavior, which has not been reported in previous papers.

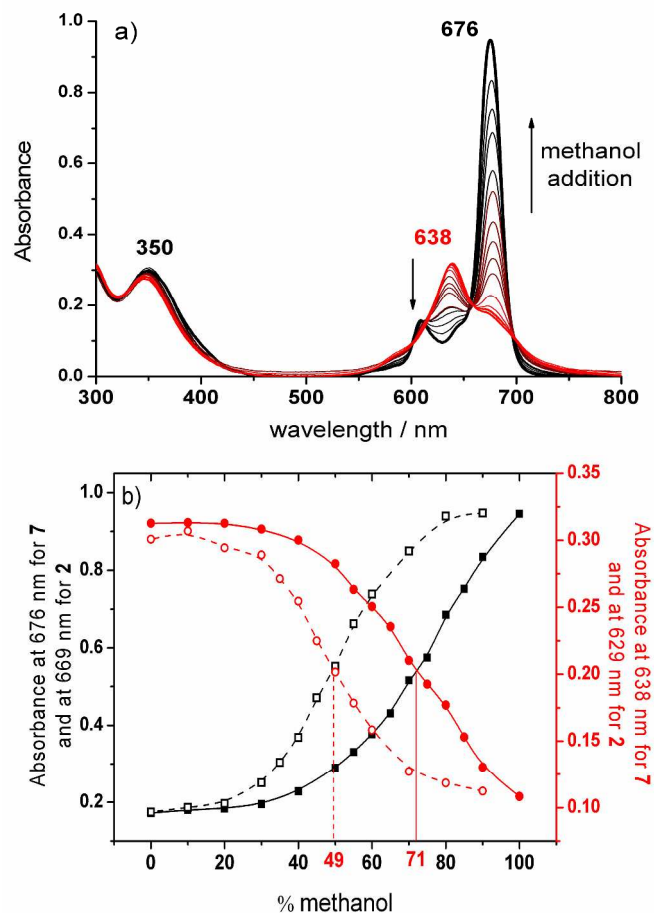


Fig. 2 (a) UV-vis absorption spectra of compound **7** in several water/methanol mixtures. (b) Solid lines: Plots of the absorbance at 676 nm (monomer band, and at 669 nm for **2** and at 638 nm for **7** and at 629 nm for **2**).

filled squares) and 638 nm (dimer band, filled circles) of **7** versus the methanol ratio in solution (data from Fig. 2a). Broken lines: Plots of the absorbance at 669 nm (monomer band, hollow squares) and 629 nm (dimer band, hollow circles) of **2** versus the methanol ratio in solution.

A similar aggregation characteristic was observed for all of the Pcs listed in Scheme 1. The absorption spectra of compounds **4-6** in a series of water/methanol mixtures are shown in Fig. 3 and those for **1-3** and **8-10** in Fig. S2-7 (ESI), with the results summarized in Table 1. As we have previously reported, bridging group-16 elements are important for shifting the Q band of the Pcs, and the pyridinium Pcs also follow this trend.¹⁰ Compounds **1** and **2** differ from compounds **3** and **7** with respect to the chalcogen atom linking the pyridyl rings to the Pc core. The Q bands of **3** (669, 691 nm) and **7** (674 nm) are red-shifted compared to those of the corresponding macrocycles containing an oxygen bridge, **1** (660, 685 nm) and **2** (665 nm), in pure methanol. This illustrates the higher electron-donating ability of the sulfur atom towards the Pc ring compared to oxygen, which leads to a larger destabilization of the HOMOs, and a resulting smaller HOMO-LUMO gap. Although the I_M values of compounds **1** (70%) and **3** (68%) are almost the same, oxygen-bridged ZnPc **2** interestingly showed a much lower value (49%) than sulfur-bridged **7** (71%). We previously determined the I_M of a pyridiniumoxy Pc cobalt(II) complex, and a low I_M value of 55% was obtained.⁷ These values are lower than both free-base pyridiniumoxy Pc **1** and pyridiniumthio Pcs **3-7**, indicating again that the extent of aggregation may result from a concomitant effect of both the bridging atoms and central metal.

Fig. 3 (a) UV-vis absorption spectrum of **4** (top), **5** (middle), and **6** (bottom) in several water/methanol mixtures; (b) plots of the absorbance values of the 674 nm (black) and 634 nm (red) bands for **4** (top), the 667 nm (black) and 628 nm (red) for **5** (middle), and the 657 nm (black) and 620 nm (red) bands for **6** (bottom) as a function of the methanol ratio in solution.

Table 1 Summary of the aggregation and emission behavior of the investigated Pcs.

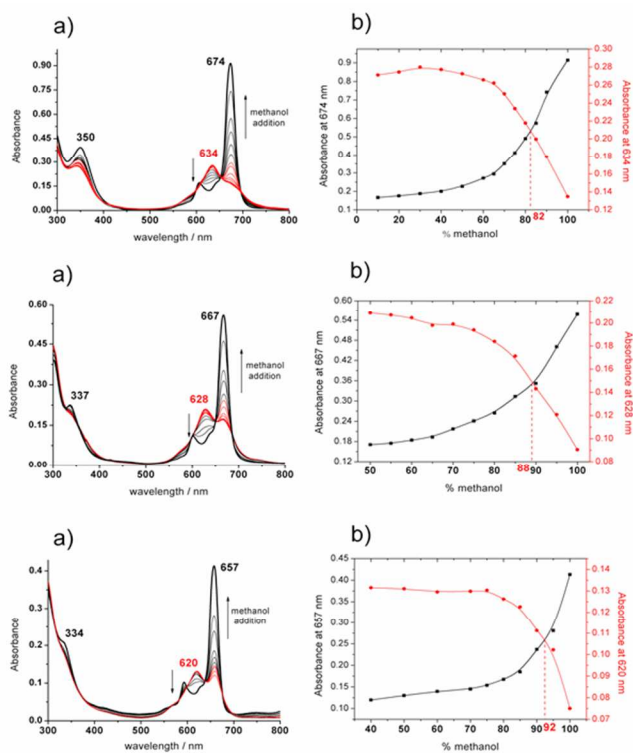
Pc	M	X	R	I_M % ^a	Abs. (nm) ^b	Em. (nm) ^c	Φ_F % ^d	
1	H ₂	O		70	660 / 685	697 / 720	15	
2	Zn			49	669	693	12	
3	H ₂	S	Methyl	68	669 / 691	706 / 740	7	
4	Cu			82	674	ND ^e	–	
5	Ni			88	667	ND	–	
6	Pd			92	657	ND	–	
7	Zn			71	674	696	15	
8				Propyl	67	677	694	14
9				Hexyl	75	675	698	12
10			Nonyl	71	675	697	13	

^a Proportion of methanol in which the monomer/dimer ratio in solution is 1:1.

^b Peaks of the Q band measured in pure methanol solution. ^c Emission peaks when excited at the Q₀₁ band in pure methanol solution. ^d Measured in pure methanol solution. ^e Not detected.

The central metal also makes a significant contribution to the stabilization of the aggregates in solution (Fig. 3). The I_M values of **4-7**, which are pyridiniumthioPc transition metal complexes, are higher than that of free-base Pc (**3**) ($I_M = 68\%$). The order is Zn (**7**) (71%) < Cu (**4**) (82%) \leq Ni (**5**) (88%) \approx Pd (**6**) (92%), with a difference in the methanol proportion of 21% between the lowest (Zn) and highest (Pd) I_M values. These results show that the metallic center makes a significant contribution to the stabilization of the aggregates in solution. ZnPc **7** has a low I_M value, indicating that it has a low propensity towards aggregation, which may be related to the 5th coordination of solvent molecules. In contrast, Cu-, Ni-, and Pd complexes are more prone to aggregation, perhaps due to the absence of a 5th coordination, so that these metalloPcs are known to form even trimers or tetramers in concentrated solution.⁶ However, the solution concentrations used in this study are of the order of 10^{-6} M, and a set of isosbestic points appeared between the spectra in water/methanol mixture and in methanol, which is monomeric. Accordingly, the spectroscopic change here is between dimer and monomer. Although it is well known that Cu complexes have a higher tendency to aggregate,¹¹ our present results show that not only Cu, but also Ni and Pd complexes, have a similar or slightly higher propensity towards aggregation.

Fluorescence measurements of the Pcs were carried out in pure methanol. The emission spectra are shown for compounds **7** and **2** in Fig. 4 and for **1**, **3** and **8-10** in Fig. S8-12 (ESI), with the results summarized in Table 1. The emission spectra are mirror images of the absorption spectra, with Stokes shifts of less than ca. 20 nm, which is in agreement with the values found for other Pcs.^{1, 12} No significant difference is observed in the emission peak wavelengths or in the fluorescence quantum yields (Φ_F) of complexes **7-10**, indicating again that the Pc electronic structure remains almost unaffected by the length of



the alkyl chain. Compounds **4-6** showed no appreciable fluorescence emission, as reported for other Ni-, Cu-, and PdPc complexes.¹ The aggregation equilibrium of the Pcs was also investigated through measurement of their Φ_F in a series of water/methanol mixtures. The excellent relationship found between the Φ_F and Q_{00} absorption intensity of the monomer clearly shows that fluorescence quenching is caused by the dimer formation with increasing proportion of water in solution. It is expected, therefore, that the solution containing a 1:1 monomer/dimer ratio will show half of the Φ_F measured in pure methanol, where the Pc is totally monomeric. In the case of **7**, the point at which the Φ_F is halved (7.5%) corresponds to the solution containing 70% of methanol, in excellent agreement with the I_M value (71%) derived from the absorbance plots previously discussed.

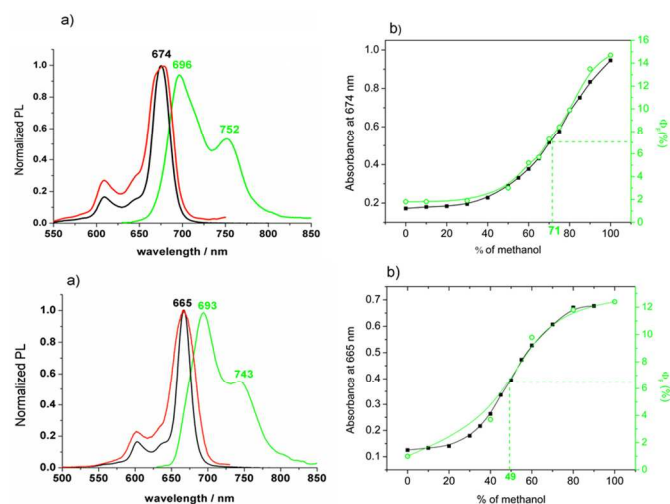


Fig. 4 (top) a) Absorption (black), fluorescence emission excited at 600 nm (green), and excitation spectra at 760 nm (red) of compound **7** in methanol solution; b) Relationship between the absorbance at 674 nm and fluorescence quantum yield of **7** upon aggregation in water/methanol mixtures. (bottom) a) Absorption (black), fluorescence emission excited at 600 nm (green), and excitation spectra at 760 nm (red) of compound **2** in methanol solution; b) Relationship between the absorbance at 665 nm and fluorescence quantum yield of **2** upon aggregation in water/methanol mixtures.

Conclusions

In summary, using quaternized pyridinium Pcs, the relationships between the Pc structure, aggregation behavior, and fluorescence intensity have been elucidated. The aggregation equilibrium depends on both the central metal and the bridging atom between the Pc core and pyridine unit. Here, the aggregation tendency increases in the order of $Zn < Cu \cong Ni, Pd$, while the bridging element sulfur gives much more propensity for aggregation compared to oxygen. We feel that it is important that the aggregation propensity can be expressed precisely using I_M values and the volumetric ratio of water in methanol-water mixtures where Φ_F becomes half of that in pure methanol. The chain length of the *N*-alkyl groups showed no significant effect on the photophysical properties or aggregation equilibrium of the Pcs in solution, so that elongation of the alkyl chain may be useful for obtaining compounds with improved amphiphilicity, without altering their intrinsic photophysical properties. We also found a noteworthy,

exemplary correlation between the fluorescence quantum yield and the extent of aggregation. These trends can be used for designing new Pc-based functional dyes for biological applications.

Acknowledgements

This work was partly supported by a Grant-in-Aids for Scientific Research on Innovative Areas (25109502, “Stimuli-responsive Chemical Species”), Scientific Research (B) (No. 23350095), Challenging Exploratory Research (No. 25620019) and Young Scientist (B) (No. 24750031) from the Ministry of Education, Culture, Sports, Science, and Technology (MEXT).

Notes and references

^a Department of Chemistry, Graduate School of Science, Tohoku University, Sendai 980-8578, Japan.

E-mail: nagaok@m.tohoku.ac.jp; Tel: +81 22 795 7719

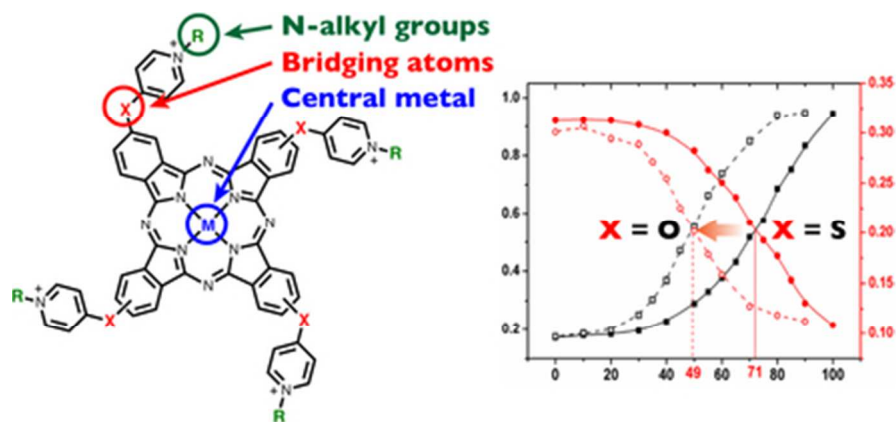
^b Department of New Business, Orient Chemical Industries, Co. Ltd., Neyagawa, Osaka 572-8581, Japan.

E-mail: y_yamasaki@orientchemical.com

† Electronic Supplementary Information (ESI) available: Experimental procedures and full details of spectra for all studied compounds. See DOI: 10.1039/b000000x/

- (a) *The porphyrin handbook*, ed. K. M. Kadish, K. M. Smith and R. Guilard, Academic Press, San Diego, 2000, vol. 1–10; *The porphyrin handbook*, ed. K. M. Kadish, K. M. Smith and R. Guilard, Academic Press, San Diego, 2003, vol. 11–20. (b) *Handbook of Porphyrin Science*, ed. K. M. Kadish, K. M. Smith and R. Guilard, World Scientific Publishing, Singapore, 2010, vol. 1–25. (c) *Phthalocyanines: properties and applications*, ed. C. C. Leznoff and A. B. P. Lever, VCH, New York, NY, 1989, vol. 1–4.
- (a) F. Dumoulin, M. Durmuş, V. Ahsen and T. Nyokong, *Coord. Chem. Rev.* 2010, **254**, 2792-2847; (b) T. Nyokong, *Coord. Chem. Rev.* 2007, **251**, 1707-1722.
- (a) M. Göksel, M. Durmuş and D. Atilla, *J. Photochem. Photobiol. A* 2013, **266**, 37-46; (b) X.-y. Li, X. He, A. C. H. Ng, C. Wu and D. K. P. Ng, *Macromolecules* 2000, **33**, 2119-2123.
- (a) M. B. Spesia and E. N. Durantini, *J. Photochem. Photobiol. B* 2013, **125**, 179-187; (b) X. Cai, M. P. Donzello, E. Viola, C. Rizzoli, C. Ercolani and K. M. Kadish, *Inorg. Chem.* 2009, **48**, 7086-7098; (c) I. Scalise and E. N. Durantini, *Bioorg. Med. Chem.* 2005, **13**, 3037-3045.
- (a) E. J. Osburn, L.-K. Chau, S.-Y. Chen, N. Collins, D. F. O'Brien and N. R. Armstrong, *Langmuir* 1996, **12**, 4784-4796; (b) X.-F. Zhang and H.-J. Xu, *J. Chem. Soc., Faraday Trans.* 1993, **89**, 3347-3351.
- A. W. Snow and N. L. Jarvis, *J. Am. Chem. Soc.* 1984, **106**, 4706-4711.
- T. T. Tasso, T. Furuyama and N. Kobayashi, *Inorg. Chem.* 2013, **52**, 9206-9215.
- M. Kasha, H. R. Rawls and M. A. El-Bayoumi, *Pure. Appl. Chem.* 1965, **11**, 371-392.
- K. Wang, D. Qi, H. Wang, W. Cao, W. Li and J. Jiang, *Chem. Eur. J.* 2012, **18**, 15948-15952.
- (a) T. Furuyama, K. Satoh, T. Kushiya and N. Kobayashi, *J. Am. Chem. Soc.* 2014, **136**, 765-776; (b) N. Kobayashi, T. Furuyama and K. Satoh, *J. Am. Chem. Soc.* 2011, **133**, 19642-19645; (c) N. Kobayashi, H. Ogata, N. Nonaka and E. A. Luk'yanets, *Chem. Eur. J.* 2003, **9**, 5123-5134.

- 11 W. J. Schutte, M. Sluyters-Rehbach and J. H. Sluyters, *J. Phys. Chem.* 1993, **97**, 6069-6073.
- 12 W. Chidawanyika, A. Ogunsiye and T. Nyokong, *New. J. Chem.* 2007, **31**, 377-384.



Good correlation between aggregation and fluorescence properties of amphiphilic phthalocyanines can be observed.

37x17mm (300 x 300 DPI)